

Aus dem Institut für Anatomie und Zellbiologie
(Prof. Dr. rer. nat. J. Wilting)
Im Zentrum Anatomie
der Medizinischen Fakultät der Universität Göttingen

Ultrastructural characterization of human thigh lymphatic collectors

INAUGURAL – DISSERTATION

zur Erlangung des Doktorgrades
der Medizinischen Fakultät der
Georg-August-Universität zu Göttingen

vorgelegt von

Viktoria Hasselhof

aus

Kiel

Göttingen 2017

Dekan: Prof. Dr. rer. nat. H. K. Kroemer

Referent: Prof. Dr. rer. nat. J. Wilting

Ko-Referent/in: Prof. Dr. Lutz Kretschmer

Drittreferent/in: Prof. Dr. Margarete Schön

Datum der mündlichen Prüfung: 24. Januar 2018

Hiermit erkläre ich, die Dissertation mit dem Titel
“Ultrastructural characterization of human thigh lymphatic
collectors” eigenständig angefertigt und keine anderen als die
von mir angegebenen Quellen und Hilfsmittel verwendet zu
haben.

Göttingen, den 04.07.2017

A handwritten signature in black ink, reading "Viktoria Janselke". The signature is written in a cursive style with large, flowing letters and a prominent flourish at the end of the last name.

Table of Contents

1 Introduction	1
1.1 The lymphatic system	2
1.2 Lymphatic vessels	3
1.2.1 Structure of the lymphatic vessel wall	4
1.2.2 Sinusoids and capillaries	4
1.2.3 Pre-collectors	4
1.2.4 Collectors	5
1.2.5 Lymph nodes	5
1.2.6 Thoracic duct	5
1.3 Development of the lymphatic vascular system	6
1.4 Purpose of my Thesis	7
2 Material and Methods	8
2.1 Devices	8
2.2 Materials	9
2.3 Chemicals	9
2.4 Reagents	10
2.5 Histology	12
2.5.1 Tissue	12
2.5.2 Light microscopy	13
2.5.3 Immunofluorescence microscopy	14
2.5.4 Transmission electron microscopy (TEM)	18
2.5.5 Photographic documentation	21
3 Results	22
3.1 Immunofluorescence verification of lymphatic collectors	22
3.2 Structure of the lymphatic collectors under the TEM	23
3.2.1 Tunica interna	24
3.2.2 Tunica media: Smooth muscle cells (SMC)	28
3.2.3 Tunica media: Vasa vasorum	30
3.2.4 Tunica media: Interstitial Cajal-like Cells (ICLC)	31
3.2.5 Tunica media: Connective tissue	35
3.2.6 Tunica externa	38
3.2.7 Fibrocytes compared to Interstitial Cajal-like Cells	40
4 Discussion	41
4.1 Mechanical concept of human lymphatic vessel contractility	41
4.2 Physiological studies	42
4.3 Immuno-histological and ultra-structural identification of ICLC	42
5 Summary	45
6 Appendix	47
6.1 List of Figures	47
6.2 List of Tables	48
6.3 List of Abbreviations	48
7 Bibliography	50

1 Introduction

The human body is constructed of many different systems working in synchrony to ensure the functionality of the human being. Over the course of human history, an abundance of research has been done to further understand these individual components. Many of the systems have been dissected, categorized and examined down to the smallest protein or transporter located in its cells' membranes. However, the lymphatic vascular system has not enjoyed as much attention as e.g. the cardiovascular system. Yet, it is a very substantial and integral part of the human body. It goes unnoticed by most people, is treated like an outcast during lectures in medical schools and if a random selection of surgeons were asked if they had ever seen its abundant components during operations, most would likely say they have not. It's when the parts of this system don't work that it is recognized and can lead to much despair in the patients.

“Lymphedema is a significant global problem, and its incidence will increase with a population that is living longer. In addition, because of the interrelationship between the lymphatic system and adipose tissue, the obesity epidemic has led to a rapid rise in this complication” (Neligan et al. 2015, p. 634). Understanding the molecular composition of the lymphatic system is essential in order to one day be able to target certain structures for therapeutic intentions. If science can come to understand what drives this system, but also what disrupts it and leads to conditions such as lymphedema, a cure or at the least, better treatment options, will more likely be found.

Over the past two decades, research on the lymphovascular system has seen some great advancements (Tammela and Alitalo 2010). However, most of the research has

been conducted in mice. Studies on lymphatic collectors were performed on animal tissues such as lymphatic ducts in canine (Todd and Bernard 1973), guinea pig (Alessandrini et al. 1981), and sheep (Hollywood and McHale 1994), and in bovine mesenteric lymphatic vessels (Allen et al. 1988). The presence of pace-maker cells has been reported in various human tissues such as human myocardium (Kostin and Popescu 2009), resting mammary gland stroma (Gherghiceanu and Popescu 2005), uterus and fallopian tube (Popescu et al. 2007), and bladder (Johnston et al. 2010), as well as in the largest part of the lymphatic vascular system, the thoracic duct (Briggs Boedtkjer et al. 2013). More specifically, Briggs Boedtkjer et al. showed pace-maker cells to be located in the outer layers of the tunica media (Briggs Boedtkjer et al. 2013).

1.1 The lymphatic system

The lymphovascular system is a specialized vascular system of the human body composed of lymphatic capillaries (initial lymphatics and lymphatic sinusoids), pre-collectors, collectors, lymph nodes, trunks and ducts filled with lymph and leukocytes (Wilting and Chao 2015). It is a distinctive vasculature starting with initial lymphatics that possess a discontinuous basement membrane, endothelial junctions that function as valves, and anchoring filaments, and proceeded by collectors with semilunar valves and intrinsic contractility (Witte et al. 2006). As a central part of the immunoregulatory network, the lymphatic vascular system is an integral part of the plasma - tissue fluid - lymph circulation known as the “blood-lymph loop” (Witte et al. 2006). Not only is the lymphovascular system a transport and immunoregulatory system, but it is also involved in diverse developmental, growth, repair and pathologic

processes (Witte et al. 2006). Interstitial fluid, chylomicrons, migrating cells and pathogens are taken up by the initial lymphatics and transported to lymph nodes via lymphatic collectors (Tammela and Alitalo 2010; Witte et al. 2001). The fluid is then carried by efferent lymphatic collectors and trunks to ultimately drain into the jugulo-subclavian venous junction. In order to create this one-way system of fluid movement, valves are regularly distributed throughout the vessels (Leak and Burke 1968; Baluk et al. 2007). It was mostly taught that the propulsion of the fluid occurred through skeletal muscle contractions and breathing. The muscles would compress the lymphatic vessels, cause the one-way valves to open under the pressure and allow a forward flow of fluid. However, it has been shown with intradermal indocyanine green (ICG) injected into the first and second interdigital space, and observation with an infrared camera, that the lymphatic vessels undergo pulsatile contractions without skeletal muscle contraction involvement (Rasmussen et al. 2009).

1.2 Lymphatic vessels

Lymphatic vessels are present in almost all tissues except for the central nervous system, the placenta, and the primary lymphatic organs (bone marrow, thymus cortex and medulla) (Rusznayk et al. 1969). Unlike the cardiovascular system, which is a continuous circulatory system (apart from the spleen and the placenta), the lymphatic vessels start off blind-ended. The movement of interstitial fluid into initial lymphatics is conducted by very fine pressure gradients and controlled by delicate lymphendothelial valves, stabilized by anchoring filaments and equipped with specialized intercellular junctions (Leak and Burke 1968; Baluk et al. 2007). Segments of the lymphatic vascular system, however, do have a similar structure to that of the cardiovascular system.

1.2.1 Structure of the lymphatic vessel wall

Many sections of the lymphatic vasculature have the same general structure as that of the cardiovascular system, in that the vascular wall consists of a tunica interna (intima), tunica media (media) and tunica externa (adventitia). Differences arise depending on the caliber of the vessels and their function.

1.2.2 Sinusoids and capillaries

Initial lymphatics (lymphatic capillaries and sinusoids), the smallest of the lymphatic vessels, are located in the adventitia of all the major blood vessels (usually arteries), but also form independent networks in the stroma of most organs (Wilting and Chao 2015). They start off blind-ended and consist only of lymphatic endothelial cells, i.e. basal lamina and pericytes are missing (Wilting and Chao 2015). The term lymphatic sinusoid is justified by the fact that the diameter of lymphatic capillaries is approximately 50 μm , which is considerably larger than that of blood capillaries (Wilting and Chao 2015). Anchoring filaments are responsible for connecting the lymphatic endothelial cells to the elastic extracellular matrix (Casley-Smith 1980). Overlapping junctions or “overlapping leaflets” interconnect the lymphatic endothelial cells and create valves that allow an influx but hinder an efflux of fluid and small particles (e.g. bacteria, viruses, leukocytes, tumor cells) (Baluk et al. 2007).

1.2.3 Pre-collectors

Pre-collectors have a diameter of appr. 100 μm and are still highly permeable (Wilting and Chao 2015). A basal lamina is rarely present on this level (Wilting and Chao 2015). Occasionally, leaflets form a “second valve system” that is comparable

to the ones found in veins (Wilting and Chao 2015). Lymphatics possess more frequent valves than the veins (Wilting and Chao 2015).

1.2.4 Collectors

Collectors are the first level to show a wall structure subdivided into intima, media and adventitia (Wilting and Chao 2015). A basal membrane is present under the endothelial cells. Collectors are also the first level to show spontaneous contractions of approximately 6-12 times per minute due to pace-maker cells and smooth muscle cells located in the media (Witte et al. 2006). Lymph may be carried 30-40 cm in the collectors before arriving at the first lymph node (Berens von Rautenfeld and Drenckhahn 1994).

1.2.5 Lymph nodes

Human bodies contain approximately 300-700 lymph nodes, which appears to be more than any other vertebrate (Wilting and Chao 2015). Lymph nodes are kidney-shaped and range in size from 1 to 25 mm. Afferent lymph enters on the convex surface whereas the hilum is located on the concave side and contains efferent lymph vessels and the lymph node artery and vein (Wilting and Chao 2015).

1.2.6 Thoracic duct

Lymph from the lymph nodes is transported through lymphatic trunks to the lymphatic ducts e.g. the thoracic duct (Berens von Rautenfeld and Drenckhahn 1994). The wall of the thoracic duct is several millimeters thick and is nourished by vasa vasorum in the adventitia. The wall contains a tunic interna with endothelial cells and lamina propria intima, tunica media and tunic externa (Wilting and Chao 2015).

1.3 Development of the lymphatic vascular system

Human embryos of 6-7 weeks of age show the presence of jugular lymph sacs. This is about 3 to 4 weeks after the first presence of the blood vascular system (Van der Putte 1975). Due to this time difference, the blood vascular system is considered to be primary and the lymphovascular system secondary. Mutations that affect cardiovascular functionality cause early embryonic death (Wilting et al. 2004). Abnormalities that affect the lymphatic vessel development however, are mostly not embryonic lethal (Wilting et al. 2004). Wilting et. al. suggested in 2004 that the first intraembryonic vessels in vertebrate embryos are lymphatic rather than cardiovascular due to their structure and the expression of a typical lymphatic endothelial receptor, VEGFR-3 (Vascular Endothelial Growth Factor Receptor-3) (Wilting et al. 2004). Much of the research on the development of the lymphatic vascular system has taken place with mice. However, Florence Sabin performed pioneering studies in the early 1900's in pigs and suggested that lymphatic vessels originate from the embryonic veins, progressively sprouting and growing centrifugally to generate an interconnected lymphatic vascular plexus (Betterman and Harvey 2016; Sabin 1902; Sabin 1904). Molecular support for Sabin's hypothesis came from detailed studies that revealed Prox1 protein localization in the embryonic veins and in the vascular structures budding from the veins and identified as lymphatic vessels (Wigle et al. 2002). In addition to lymphatic cells sprouting from the veins to form lymphatic sacs that remodel into vessels; in embryonic dermis, heart and mesentery, alternative sources of progenitor cells have been documented to contribute to the development of the lymphatic vasculature (Betterman and Harvey 2016). These two systems arise independently and progressively proliferate, migrate and coalesce to form interconnected vessels (Betterman and Harvey 2016). The lymphatic vasculature

matures through a process of remodeling the initial lymphatic vascular plexus into a network of initial, pre-collector and collecting vessels; recruiting vascular smooth muscle cells and pericytes to the walls of precollector and collecting vessels; and developing lymphatic vessel valves in pre-collector and collecting vessels (Betterman and Harvey 2016).

1.4 Purpose of my Thesis

Human lymphatic collectors are not well characterized, both at morphological and molecular level. The few existing morphological studies have focused on the thoracic duct of the human (Briggs Boedtkjer et al. 2013) or lymphatic vessels of animals (Sabin 1902; McCloskey et al. 2002; Todd and Bernard 1973).

The focus of this thesis is to characterize epifascial human lymphatic collectors at the transmission electron microscopic (TEM) level, and thereby also determine if pacemaker cells existed in lymphatic collectors as they have been reported to exist in the thoracic duct. Tissue was collected from patients with healthy thigh lymphatic collectors being collected for lymph vessel transplantation to the arm after breast cancer therapy and axillary revision. Immunohistology was used to confirm the lymphovascular nature of the collected tissue. Once confirmed, specimens were studied with TEM for characterization of the cellular composition and ultrastructure of the collectors. A precise understanding of the cellular components of lymphatic collectors is essential for any further research that should ultimately lead to therapeutic procedures, e.g. the treatment of lymphedema.

2 Material and Methods

2.1 Devices

- Centrifuges: Refrigerated Centrifuge (5417R): Eppendorf, Hamburg, Germany
Table mini centrifuge Model GMC 060: LMS Co., LTD, Japan
- Microscopes: Electron microscope (906 E): Leo Elektronmikroskopie GmbH,
Oberkochen, Germany
Immunfluorescence microscope (LEICA DM 5000 B): Leica,
Bensheim, Germany
Light microscope: Zeiss, Jena, Germany
Photo microscope: Zeiss, Jena, Germany
Stereo microscope: Wild, Heerbrugg, Switzerland
- Miscellaneous: Autoclave (type 23): Melag Medizintechnik, Berlin, Germany
Automated slide stainer (Stainette E 7751): Shandon, Frankfurt/M.,
Germany
Camera: LEICA Microsystems DI Cambridge (B1), Great Britain
Cryotome LEICA CM 30505: Leica, Bensheim, Germany
Diamond knife (type MS 3518): Diatome, Heidelberg, Germany
Digital camera (CCD Camera KP-M2E/K): Hitachi Denshi, Ltd.
Japan
Digital scale: Sartorius, Göttingen, Germany
Dissecting set: Aesculap, Tuttlingen, Germany
Embedding station (Histokinette 2000): Reichert-Jung, Heidelberg,
Germany
Fluorescence lamp: Leistungselektronik Jena GmbH, Jena,
Germany
Heating block: Neolab, Heidelberg, Germany
Heating plate: Schütt, Göttingen, Germany
Incubator (Modell 200): Memmert, Schwabach, Germany

Microtome (Jung-Biocut-2035): Leica, Nussloch bei Heidelberg, Germany

Paraffin cold plate: Shandon, Frankfurt/M., Germany

Photometer: Dynatech MR 5000, Denkendorf, Germany

Photoscanner (Scann 2000): Praktika, Wiesbaden, Germany

Refrigerator: Liebherr Hausgeräte, Ochsenhausen, Germany

Ultramicrotome (Ultracut): Reichert-Jung, Heidelberg, Germany

Vortexer: Schütt, Göttingen, Germany

2.2 Materials

Copper slit aperture	Plano, Wetzler, Germany
Coverslip	Menzel-Gläser, Braunschweig, Germany
Disposable gloves	Hartmann, Heidenheim, Germany
Eppendorf micro test tube	Eppendorf, Hamburg, Germany
Eppendorf pipettes	Eppendorf, Hamburg, Germany
Erlenmeyer flask	Schott, Mainz, Germany
Filter paper (Whatman No.1)	Whatmann International Ltd., Maidstone, England
Glass strip (400x25x6,4mm)	Leica, Hamburg, Germany
Parafilm	American National Can co., Greenwich CT, USA
Petri dishes	Schott, Mainz, Germany
pH-meter	WTW, Weilheim, Germany
Physio care pipettes	Eppendorf, Hamburg, Germany
Pipette tips	Eppendorf, Hamburg, Germany
Slides	Knittel Glas, Braunschweig, Germany
Superfrost slides	Menzel-Gläser, Braunschweig, Germany

2.3 Chemicals

1,2-Dichlorethane	Merck, Darmstadt, Germany
Alcohol 100%	C.G.-Chemikalien Hannover, Germany

	and Epon B are mixed in a ratio of 6:4. 100 ml of this mixture is combined with 30 ml 1.8 % DMP (2,4,6-Tris(dimethylaminomethyl)phenol) as an accelerator.
Formbar solution	0.6 g polyvinyl formal is mixed with 200 ml 1,2-dichlorethane.
Karnovsky solution	10 g paraformaldehyde is mixed with 100 ml aq. dest. and stirred at 60 °C for 1 hour. 1-2 drops of NaOH are added. The solution is filtered after cooling off. Directly before using the solution, 30 ml of this 10 % paraformaldehyde solution is mixed with 58 ml 0.3M Sörensen phosphate buffer and 12 ml 25 % glutaraldehyde.
Lillies buffered formalin	4 g monosodium phosphate ($\text{NaH}_2\text{PO}_4 \times \text{H}_2\text{O}$) and 6.5 g water-free disodium phosphate (Na_2HPO_4) are mixed in 900 ml aq. dest. After the addition of 100 ml 35 % formalin, 1N HCL is used to achieve a pH of 7. Storage in a refrigerator at 4 °C.
1% Osmium tetroxide	2 % OsO_4 and 0,3 M Phosphate buffer mixed in a 1:1 ratio
Reynolds lead citrate	1.33 g lead nitrate ($\text{Pb}(\text{NO}_3)_2$) and 1,76 g sodium citrate ($\text{Na}_3(\text{C}_6\text{H}_5\text{O}_7)\text{xH}_2\text{O}$) are added to 30 ml aq. dest. and shaken vigorously for 1 minute. The solution is stored in a dark room for 30 minutes to allow the transition to lead citrate. Afterwards, 8 ml of NaOH are added to the solution. Finally, the solution is filled up to a total of 50 ml using distilled water and filtered.
Richardson solution	Two parts 1 % azur II (in distilled water), one part 2 % methylene blue (in distilled water) and 1 part 2 % borax (in distilled water) are mixed and filtered.

Sörensen phosphate buffer	The 0.3 M buffer is made by mixing 18.2 ml NaH_2PO_4 solution (41.37 g/l) and 81.8 ml Na_2HPO_4 solution (42.58 g). Using distilled water, a 0.15 M solution can be produced by adding 100 ml distilled water.
Uranyl acetate	1 g Uranyl acetate is mixed with 100 ml distilled water and filtered. It is usable for 14 days if kept at 4 °C. The solution is weakly radioactive.

2.5 Histology

2.5.1 Tissue

The human tissue used for the research of this thesis was obtained from patients suffering from secondary lymphedema of the arm after standard treatment for breast cancer including axillary revision, and undergoing autologous lymphatic collector transplantation. A healthy lymphatic collector was surgically removed from the patient's thigh hypodermis. It was consequently transplanted into the axillary region, where it was connected proximally and distally to the local lymphatic collectors as described previously (Felmerer et al. 2012). Patent Blue® was injected intradermally into the first and second interdigital space in order to identify the collectors of the patient's thigh. Once identified, an adequate section of a collector was isolated and resected. The removed section was used for the transplantation. The thigh lymphatic collector free ends were sealed. Surplus tissue not used for the transplantation, usually short end-pieces less than 1 cm long, were used for this thesis, and additional research projects (n = 21). The operations proved to be extremely successful. None of the patients developed lymphedema in the leg from which the transplant was resected. Significantly less lymphedema was observed in the patient's arm after the transplant

operation. The clinical data of these patients will be published in a separate study. This thesis was approved by the ethics committee of the University Medical Center Göttingen (application no. 11/4/05 and 5/11/06), and all patients were informed and gave their written consent.

2.5.2 Light microscopy

Tissue for light microscopy was fixed in formalin and embedded in paraffin. Afterwards, sections were prepared and stained with hematoxylin-eosin.

2.5.2.1 Fixation and embedding

Tissue was fixed in 3.7 % buffered formalin solution for 24 hours at 4 °C. It was then transferred into 70 % and 80 % ethanol. Tissue was subsequently dehydrated in an ascending ethanol concentration solution series. It was then transferred to xylene and embedded in paraffin.

2.5.2.2 Preparation of sections

Paraffin blocks were inserted into the microtome. Sections of 5 µm thickness were cut. A drop of distilled water helped transfer the section to a slide. The slide was placed on a hot plate, which was heated to a temperature between 39-42 °C. The microtome, hot plate and instruments were repeatedly cleaned with xylene and 70 % ethanol throughout the procedure. The slides were placed into an incubator at 37 °C for 24 hours. Afterwards, slides were stored in a dust free box.

2.5.2.3 Hematoxylin stain

The hematoxylin-eosin stain was performed using the following sequence:

xylene	5 min
xylene	5 min
absolute ethanol	2 min
96 % ethanol	2 min
80 % ethanol	2 min
60 % ethanol	2 min
distilled water	2 min
Mayer's hematoxylin	4 min
distilled water	1 min
running water	15 min
eosin	7 min
distilled water	1 min
60 % ethanol	1 min
80 % ethanol	1 min
96 % ethanol	1 min
absolute ethanol	2 min
absolute ethanol	2 min
xylene	3 min

Table 1: Sequence for hematoxylin-eosin stain

2.5.3 Immunofluorescence microscopy

2.5.3.1 Preparation of cryo-blocks

Specimens for immunofluorescence studies were fixed in 4 % paraformaldehyde (PFA) for 20-25 minutes. Afterwards, the specimens were rinsed in PBS and transferred into 10 % and 30 % sucrose in PBS. Finally, specimens were embedded in

tissue freeze medium (Tissue Tek, Sakura Finetek, Zoeterwoude, NL). The specimens were put into the Cryostat at -20 °C to harden. Afterwards, the blocks were wrapped in aluminum foil, numbered and stored in a freezer at -80 °C until used for research.

2.5.3.2 Preparation of frozen sections

The Cryomikrotom compartment was set to -20 °C. The specimens were cut into 14 µm thick slices. Three slices were placed on each Superfrost-slide. The slides were air dried for at least 1 hour at room temperature if directly used for staining; otherwise, they were stored at -20 °C in a box placed in the Cryostat.

2.5.3.3 Standard solutions for immunohistology

BSA: 1 % Bovine Serum Albumin

PPB: 0.2 M Potassium Phosphate buffer

27.2 g Monopotassium Phosphate (KH_2PO_4)

34.836 g Dipotassium Phosphate (K_2HPO_4)

add distilled water to reach 800 ml

add 1 N NaOH to achieve a pH of 7.3 (ca. 100 ml)

add distilled water to reach 1 L

PBS: 0.1 M Phosphate-buffered saline

72.0 g Sodium chloride

14.8 g Disodium phosphate

4.3 g Potassium hydrogen phosphate

add 1000 ml distilled water; pH 7.2

Mounting medium: Fluoromount-G (Southern Biotechnology Associates, Birmingham, GB)

2.5.3.4 Immunofluorescence antibodies

The following list of the antibodies was used in my study. The ratio for dilution with 0.1 M PPB solution is noted in brackets.

Primary antibodies:

CD31: mouse-anti-human CD31 (1:50, BD Pharmingen)

Prox-1: rabbit-anti-human Prox 1 (1:500, ReliaTech, Braunschweig, Germany)

Dapi: invitrogen molecular probes nucleic acid stain

Secondary antibodies:

Alexa Fluor 488: goat-anti-mouse Ig (1:200, Molecular Probes)

Alexa Fluor 594: goat-anti-rabbit Ig (1:200, Molecular Probes)

2.5.3.5 Immunofluorescence staining

Day 1

1. Slides were left to dry for 1 hour at room temperature
2. A humidified chamber was assembled with damped paper towel placed at the bottom of the chamber box
3. Control section was separated from other sections with grease pencil
4. Date and antibodies were labeled on slide
5. 100 μ l BSA buffer per slide was distributed onto three sections at room temperature for 1 hour
6. Slides were gently tapped on paper towel to absorb excess solution
7. 100 μ l antibody solution per slide was prepared to correct dilution
 - i. Antibody solution was centrifuged for 10 seconds
 - ii. Antibody amount was pipetted into micro-test-tube and antibody solution was diluted to above-mentioned ratios with BSA/PBS-solution.
 - iii. Solution was mixed on Vortex for a few seconds
8. Control section covered with BSA/PBS-solution
9. Other sections covered with antibody solution
10. Slides placed into refrigerator at 4 °C overnight

Day 2

1. Slides washed in 0.1 M PPB solution
2. Secondary antibodies centrifuged and Dapi solution teetered
3. Secondary antibodies diluted to above mentioned ratio using BSA/PBS-solution with 1 μ l Dapson/100 μ l added
4. Slides gently tapped on paper towel to absorb excess solution
5. Antibody-Dapi-solution distributed evenly on all sections
6. Allowed to react for 1 hour in room temperature
7. Slides washed in 0.1 M PPB solution
8. Wet slides placed on table and sections covered with Fluoromount and a cover slip
9. Slides stood up on paper towel to allow absorption of extra fluid
10. Slides allowed to dry in a dark cabinet
11. Slides arranged in slide folder for protection

2.5.4 Transmission electron microscopy (TEM)

Tissue for analysis with the transmission electron microscope were fixed in Karnovsky-solution (containing formaldehyde and glutaraldehyde) and embedded in Epon. Semi-thin sections were prepared for orientation. The ultra-microtome was used to prepare the ultra-thin sections used with the TEM. These ultra-thin sections were contrasted with uranyl acetate and lead citrate.

2.5.4.1 Fixation and embedding

Tissue was put into Karnovsky-solution overnight. The following day, the tissue was washed for 10 minutes in 0.15 M phosphate buffer. It was then placed into 1 % OsO₄-solution (solvent: 0.15 M phosphate buffer) at 4 °C for 90 minutes. The rinse with 0.15 M phosphate buffer was repeated. The tissue was then dehydrated through an ascending ethanol series (30 %, 50 %, 70 %, 90 %, 100 %, 100 %) at 4 °C, each for 10 minutes. The dehydration was followed by incubation twice for 15 minutes in propylene oxide. The tissue was then incubated in a mixture of Epon and propylene-oxide (1:1) for 1 hour at 4 °C. This was proceeded by an infiltration in Epon-propylene-oxide mixture (3:1) for 16 hours at 4 °C. The final mixture was then inserted into Teflon covered forms and covered with Epon. It was subsequently polymerized in a compartment drier for 24 hours at 60 °C.

2.5.4.2 Preparation of glass blade

A glass strip (40 cm long, 4 cm wide and 0.6 cm thick) was cleaned with ethanol. It was then set into the knife cutter. The glass was scratched using a diamond knife and then controllably cracked. A quadratic piece with a side length of 25 mm was produced. This piece was scratched diagonally and separated. The final product was a triangle with a 0.6 mm long cutting edge. Tape was used to form a water basin behind the cutting edge in order to catch the freshly cut sections. This was completely sealed using nail polish.

2.5.4.3 Preparation of semi-thin sections

A 1 µm thick section was cut for orientation. To do so, the epon block was inserted into the specimen holder. Under a binocular microscope, the block was cut into a pyramidal shape with a razor blade. The tip of the pyramid was removed to create a ca. 1 mm x 2 mm square surface. The block was then removed and inserted into the specimen holder of the Ultracut microtome. 1 µm thick sections were cut in series. A glass rod was used to collect the floating sections in the water basin. The sections were transferred to a slide and covered with a drop of distilled water. The slide was placed on a hot plate at 60 °C for about 3 minutes to dry. The slides were stained with Richardson solution and dried. The finished slide was evaluated under the light microscope.

2.5.4.4 Preparation of ultra-thin sections

Specimens were cut to a size of about 0.5 mm x 0.5 mm under the binocular microscope. Using an Ultracut microtome and diamond knife, sections of 60 nm-80 nm thickness were automatically cut. The freshly cut sections were transferred to copper slit apertures. These were coated with Formvar-film. This was done by taking dust free and alcohol cleaned slides that were roughed on three sides with a razor and submerged in 0.3 % Formvar solution. They were then dried and submerged in a Petri dish filled with distilled water to detach the film. Copper apertures were placed on the film. The apertures were then lifted with parafilm foil and dried.

2.5.4.5 Contrasting of ultra-thin sections

After a minimum drying time of 30 minutes, the copper apertures were contrasted using the following table:

uranyl acetate	10 min
distilled water	thoroughly washed
lead citrate	10 min
distilled water	thoroughly washed

Table 2: Contrast sequence for copper apertures

The apertures were dried for a minimum of 30 minutes before being viewed under the Leo 906E electron microscope.

2.5.5 Photographic documentation

Production of light microscopic pictures was done with a light microscope connected to a photo scanner.

Production of electron microscopic pictures was done with the Leo 906E electron microscope with an integrated camera.

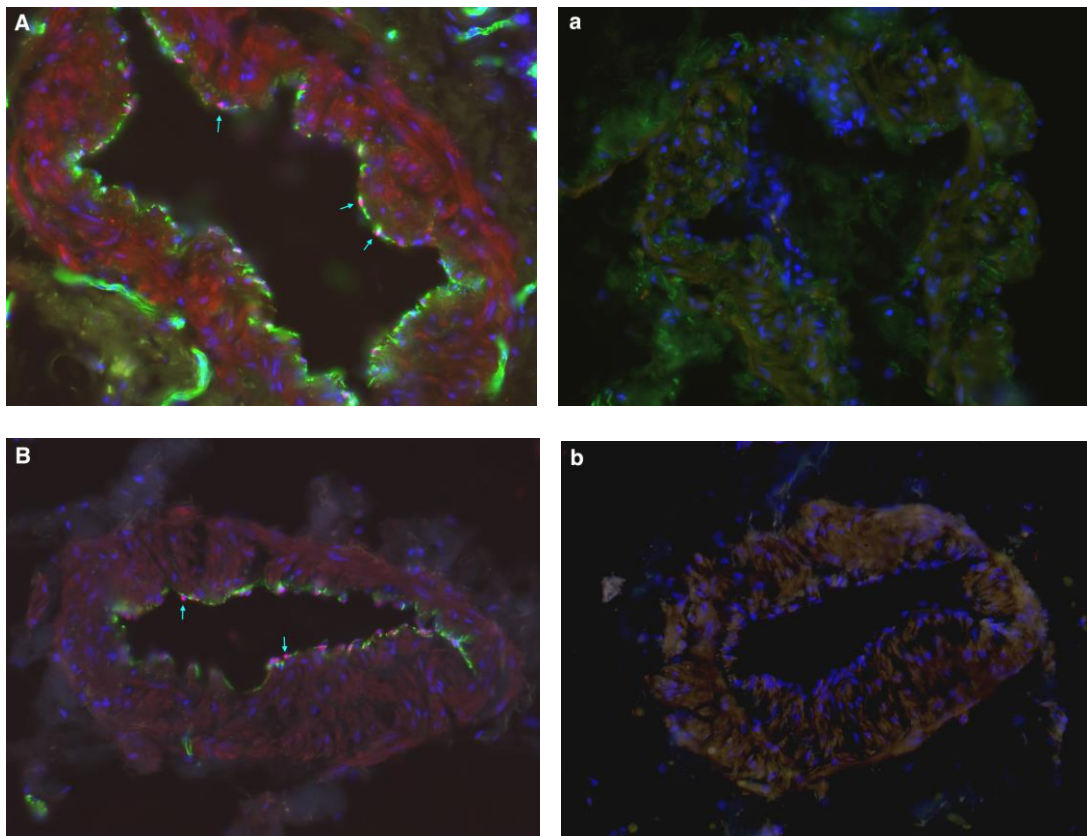
Immunofluorescence pictures were taken with a microscope LEICA DM 5000 B through stimulation of the antibodies with the appropriate light wavelengths and integrated AxioImagerZ1 camera (Zeiss, Göttingen, Germany).

Photos were worked on with a MacBook Air computer and Photos (Version 1.3 [350.23.0] Copyright 2015 Apple Inc.).

3 Results

3.1 Immunofluorescence verification of lymphatic collectors

The collected tissue was confirmed as lymphatic through a double immunofluorescence staining with antibodies against Prox-1 and CD31 (Wilting et al. 2002). Double-positivity of the endothelial cells proved the correct characterization. Although collectors varied in diameter, all collectors' luminal endothelial cells stained positively for both antibodies (**Fig. 1**).



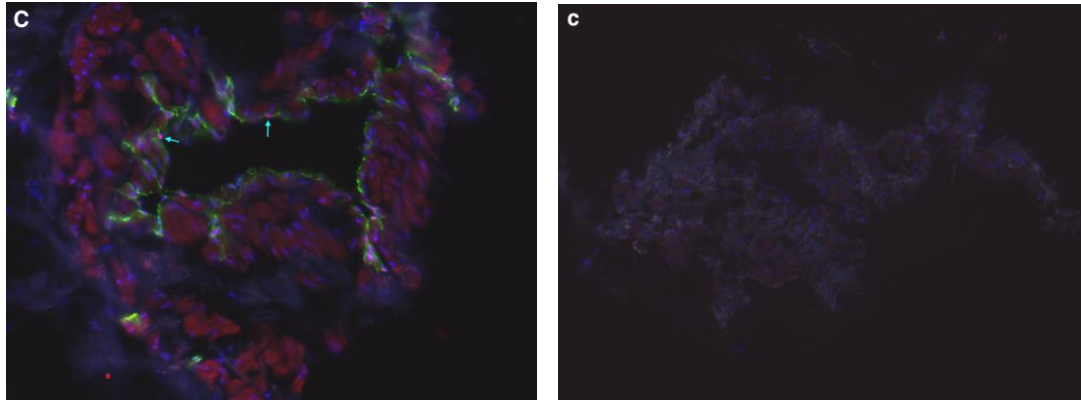


Fig. 1: Immunofluorescence studies of epifascial lymphatic collectors from the human thigh. Staining with antibodies against CD31 (green) and Prox-1 (red) (A-C), and negative control with only secondary antibodies (a-c). Lymphatic endothelial cells express both of the markers (arrows). All images are shown at 20 x objective magnification.

3.2 Structure of the lymphatic collectors under the TEM

The general structure of the lymphatic collector is similar to that of other vascular channels - tunica interna, tunica media and tunica externa. The lumen of the lymphatic collectors varied in shape. Some were fixed with a round open lumen, while others were collapsed or contracted into a more star-shaped form. The intima consisted almost exclusively of lymphatic endothelial cells (LECs). The media contained smooth muscle cells (SMCs). The collectors of larger diameter showed a thick inner predominantly longitudinally oriented layer and a thinner outer predominantly circular oriented layer of SMCs. The SMC layers were surrounded by an adventitia. Pace-maker cells were located mainly in the outer parts of the SMC layers. Media-penetrating *vasa vasorum* were also observed.

3.2.1 Tunica interna

Lymphatic endothelial cells (LECs) lined the lumen of the lymphatic collectors. They were found to be delicate and rested on a basal lamina. Unlike what is typically found in larger blood vessels, the LECs in the lymphatic collectors were usually not resting on a layer of sub-endothelial tissue but rather were in close contact with the smooth muscle cells (SMCs). The nucleus protruded into the lumen. The more contracted the lymphatic vessel was at the time of fixation, the further into the lumen the nucleus appeared to protrude. Fine processes projected into the lumen as well as towards the media. Neighboring cells either simply overlapped or created complex interdigitation (**Figs. 2 - 5**). A sub-endothelial layer of connective tissue, as observed in larger blood vessels, was not consistently observed in the lymphatic collectors.

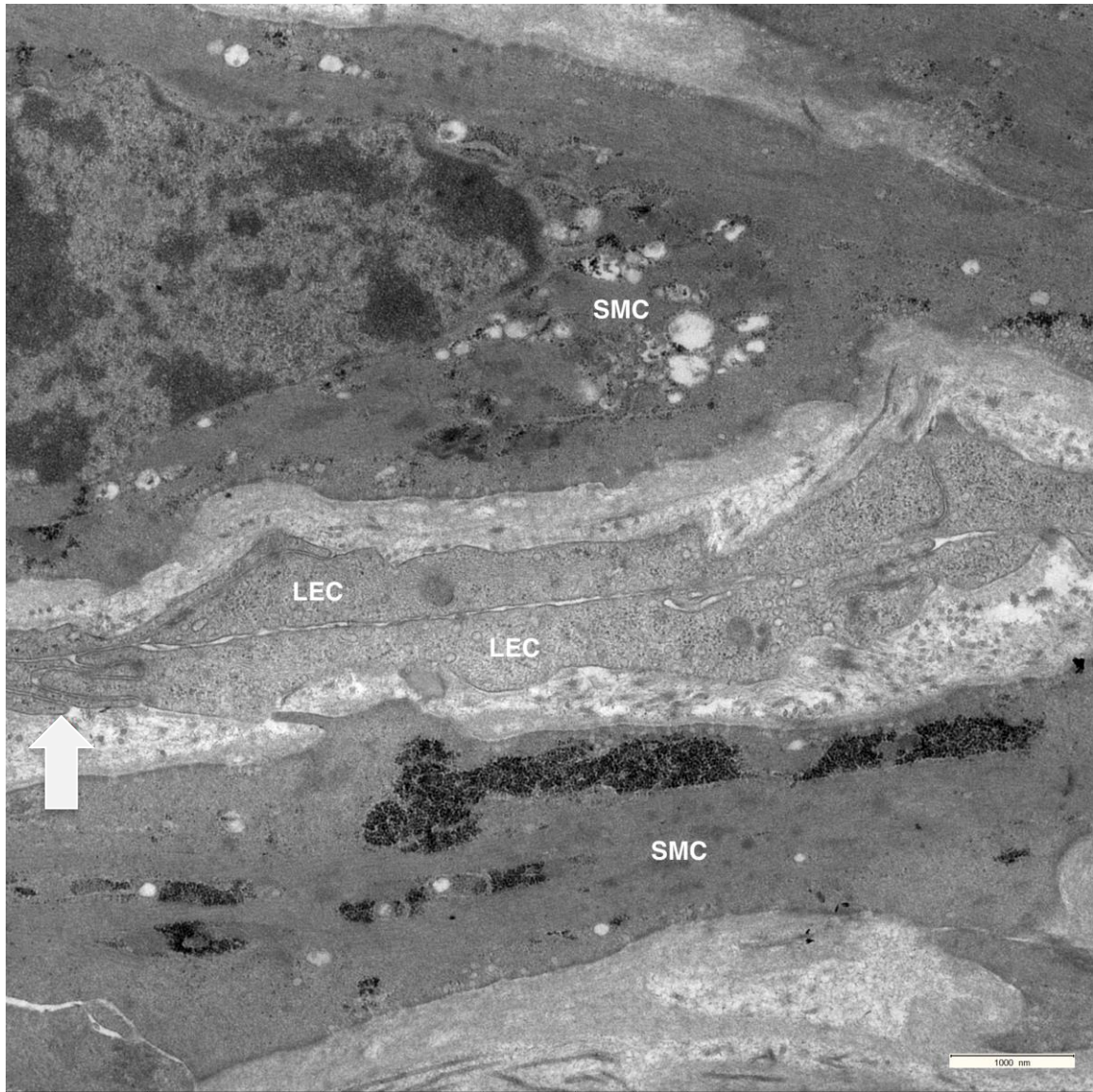


Fig. 2: TEM studies of epifascial lymphatic collector endothelial cells. Lymphatic endothelial cells (LECs) line the collapsed lumen. Endothelial cells are flanked by smooth muscle cells (SMCs). Note the interdigitations of neighboring endothelial cells (arrow). Bar = 1000 nm

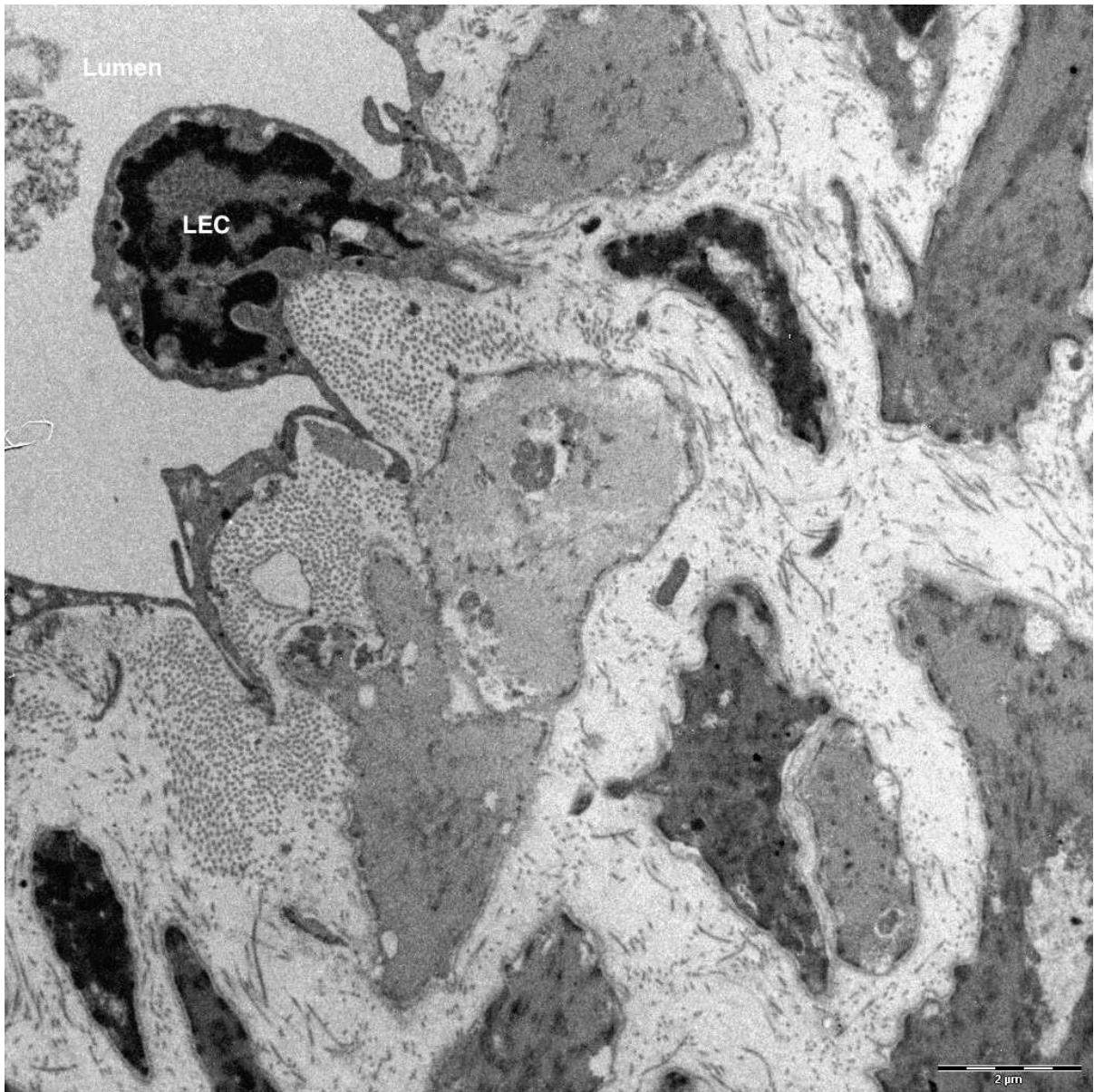


Fig. 3: Ultra-thin section of human epifascial lymphatic collector endothelial cell

TEM picture showing a lymphatic endothelial cell (LEC) protruding into the lumen with most of the cell body volume. Note the presence of light and dark colored smooth muscle cells. Bar = 2 μ m

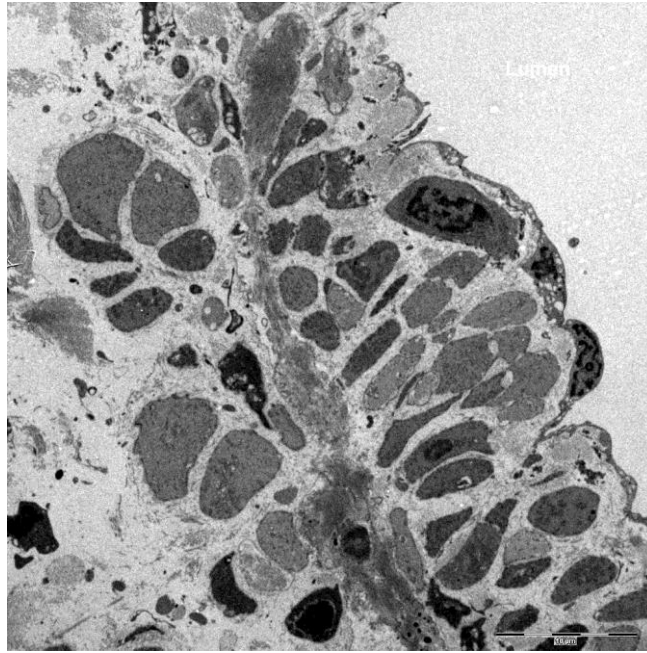


Fig. 4: Ultra-thin section of human epifascial lymphatic collector
TEM picture showing a thinner collector with only a few layers of SMC. Note the LEC and the protrusion of its cell body into the lumen. Bar = 10 μ m

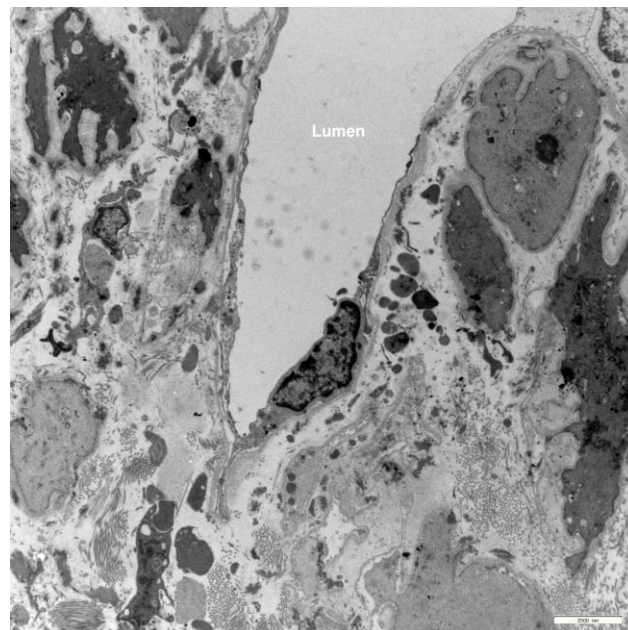


Fig. 5: Magnified ultra-thin section of human epifascial lymphatic collector endothelial cell
TEM picture showing a LEC with a more flattened cell body lining the lumen compared to previous pictures. Bar = 2500 nm

3.2.2 Tunica media: Smooth muscle cells (SMC)

The SMC layer varied in thickness amongst the specimens (varying from 200 to 600 μm). The collectors of greater diameter showed a thick inner layer of predominantly longitudinally oriented SMCs, and a thin outer predominantly circular oriented layer of SMCs. Two types of SMCs were observed with light and dark cytoplasm (**Fig. 6**). Both types possessed typical features of SMCs; basal lamina, caveolae, dense bodies, scarce mitochondria and central nucleus. The nucleus was surrounded by a complete nuclear membrane. Heterochromatin was concentrated towards the periphery of the nucleus and sparsely seen in the center. The extra-fibrillar cytoplasm was mostly restricted to the area directly around the nucleus. Mitochondria were generally scarce in the SMCs and were found in the extra-fibrillar cytoplasm at the poles of the nucleus or scattered singularly throughout the myofilaments. Myofilaments found in the SMCs included thick, intermediate and thin filaments. The thickness and density of the muscle cells varied. Many of the SMCs had fine processes to the extent of having a starfish morphology. These processes were often observed to penetrate the basal lamina of both SMCs and LECs. Rivet-like contacts between the processes and LECs or SMCs were observed (**Fig.7A**). Many SMCs had blunt projections, which made contact with neighboring cells. (**Fig.7B**) Each smooth muscle cell was fringed by a fine granular layer. Collagen, fine granular material and elastic fibers were located between the muscle cells. In some areas, the muscle cells were closely packed, while in others, they were more widely spread out.

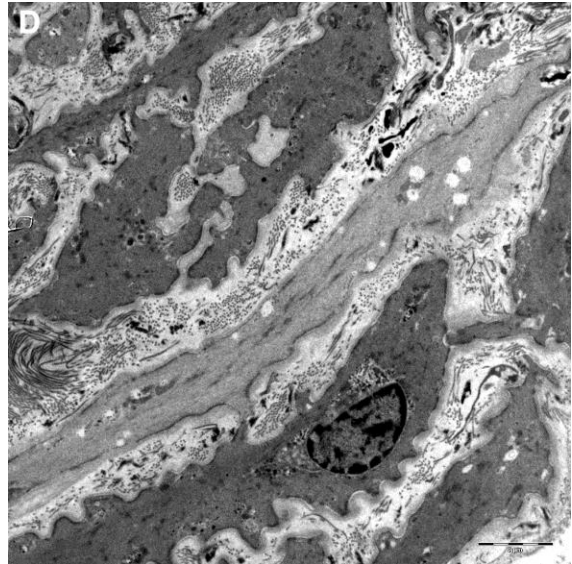
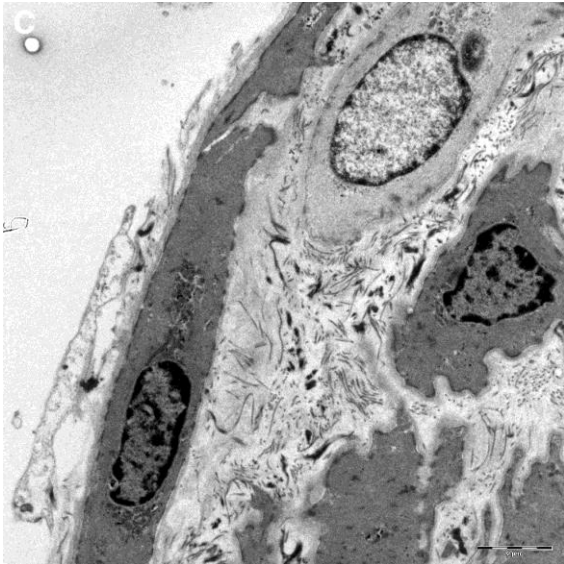
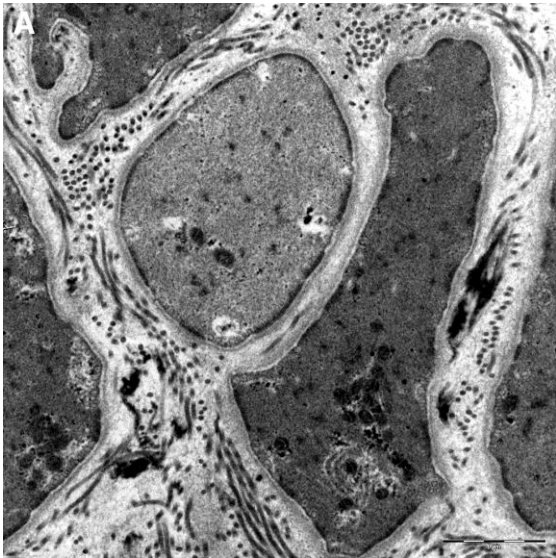


Fig. 6: Ultra-thin sections of human epifascial lymphatic collectors smooth muscle cells (SMCs)

TEM pictures showing the media with SMCs of light and dark cytoplasm. The majority have a dark cytoplasm. (A) Bar = 1 μm , (B - D) Bar = 2 μm .

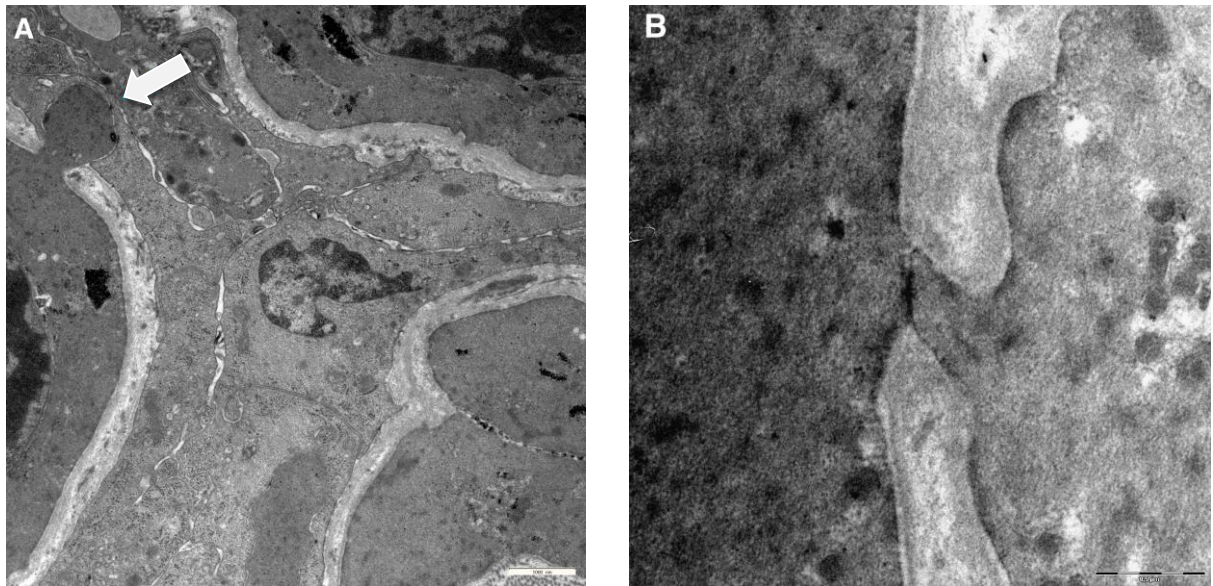


Fig. 7: Ultra-thin sections of human epifascial lymphatic collector LEC/SMC and smooth muscle cell connections

A) TEM picture showing the rivet-like connection (arrow) between the lymphatic endothelial cell and a SMC. Bar = 1000 nm **B)** TEM pictures of smooth muscle cells in the media of a lymphatic collector. Note the desmosomal connection of the SMCs. Bar = 0,5 μ m

3.2.3 Tunica media: *Vasa vasorum*

Boggon and Palfrey previously described the presence of *vasa vasorum* in the adventitia of lymphatic collectors (Boggon and Palfrey 1973). My data however clearly showed *vasa vasorum* located between SMCs in the media. They consisted of capillaries with pericytes ensheathed in a common basal lamina (**Fig. 8**). The lumen was often filled with erythrocytes. I also observed single vascular SMCs in the Media of *vasa vasorum*, indicative of a metarteriole.

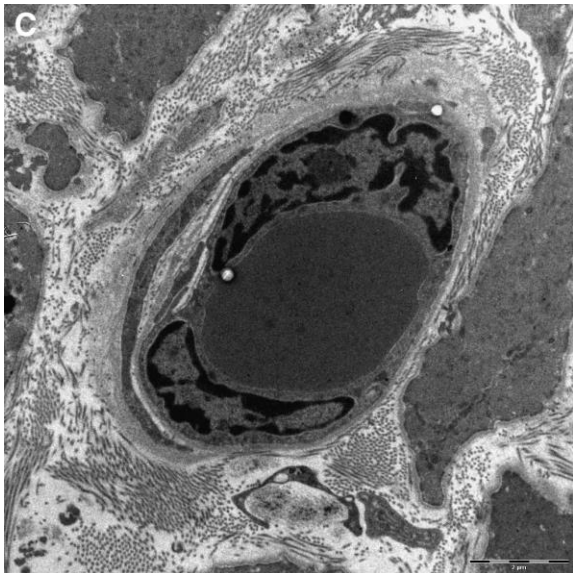
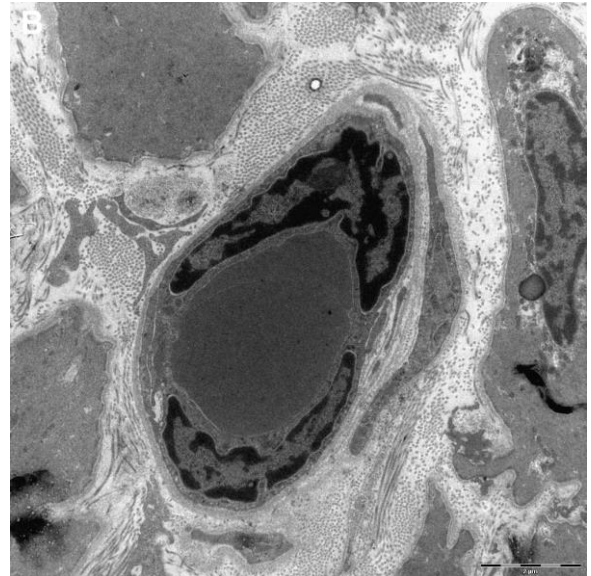
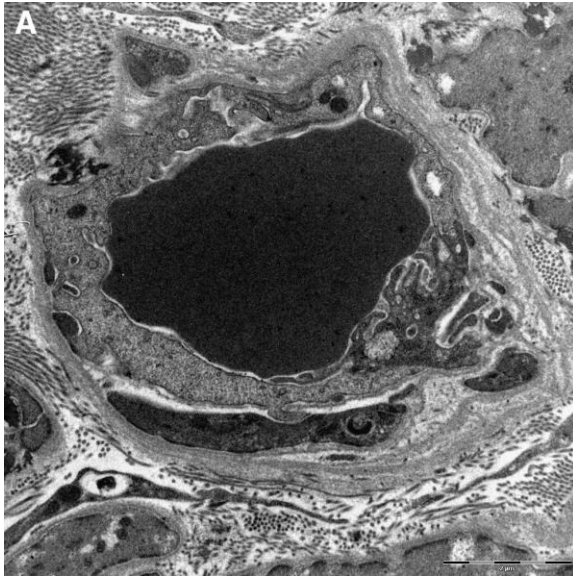


Fig. 8: Ultra-thin sections of human epifascial lymphatic collector vasa vasorum.

All three pictures depict vasa vasorum located in the media of lymphatic collectors consisting of endothelial cells and pericytes. The lumen is filled with erythrocytes.

(A),(B),(C) Bar = 2 μ m

3.2.4 Tunica media: Interstitial Cajal-like cells (ICLC)

Interstitial Cajal-like cells (ICLCs) were identified throughout the tunica media. Ultra-structurally they were characterized as ramified cells whose nucleus was surrounded by a slender perinuclear body and an indented nucleus. They contained a low amount of caveolae and, most characteristically, they possessed long cytoplasmic processes (**Figs. 9 - 11**). These processes varied in caliber, often suddenly becoming

very thin e.g. close to the cell body. They were very long and often in close contact with SMCs, where they contained dilations (**Fig. 10**). These dilations have been described as Ca²⁺-handling units, containing caveolae, ER and mitochondria (Kostin and Popescu 2009). The areas of close contact between ICLCs processes and SMCs showed a dense facing with caveolae at the contact sites (**Fig. 10B, 10D**). Caveolae have many functions, amongst others; mechanosensing, lipid regulation, endocytosis, transcytosis, and calcium signaling (Parton and Simons 2007). Potentially, the contraction of the collector could be regulated by interactions between caveolae of ICLCs and SMCs. The ICLCs as such were connected to one another through close apposition. A patchy basal lamina was not observed as described in studies on the thoracic duct (Briggs Boedtkjer et al. 2013).

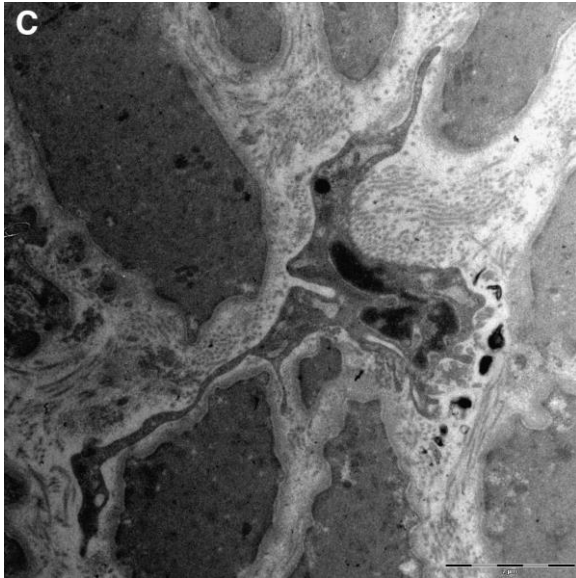
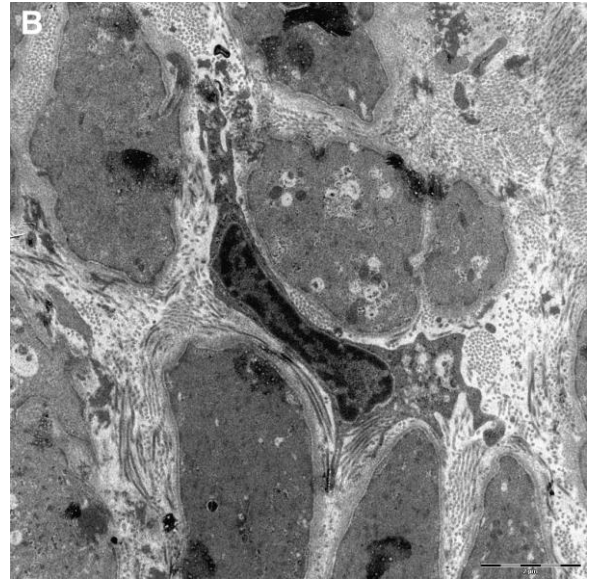
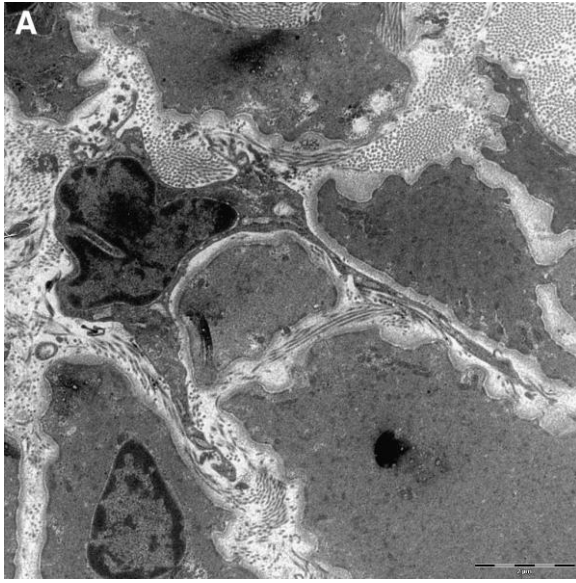


Fig. 9: TEM studies of ICLCs in the media of lymphatic collectors.

A-C) ICLC cell bodies located in the media of lymphatic collectors. Note the indented nucleus, slender cell body and long processes that become very thin close to the cell body. ICLCs are surrounded by SMCs and connective tissue.

Bar = 2 μ m in A-C

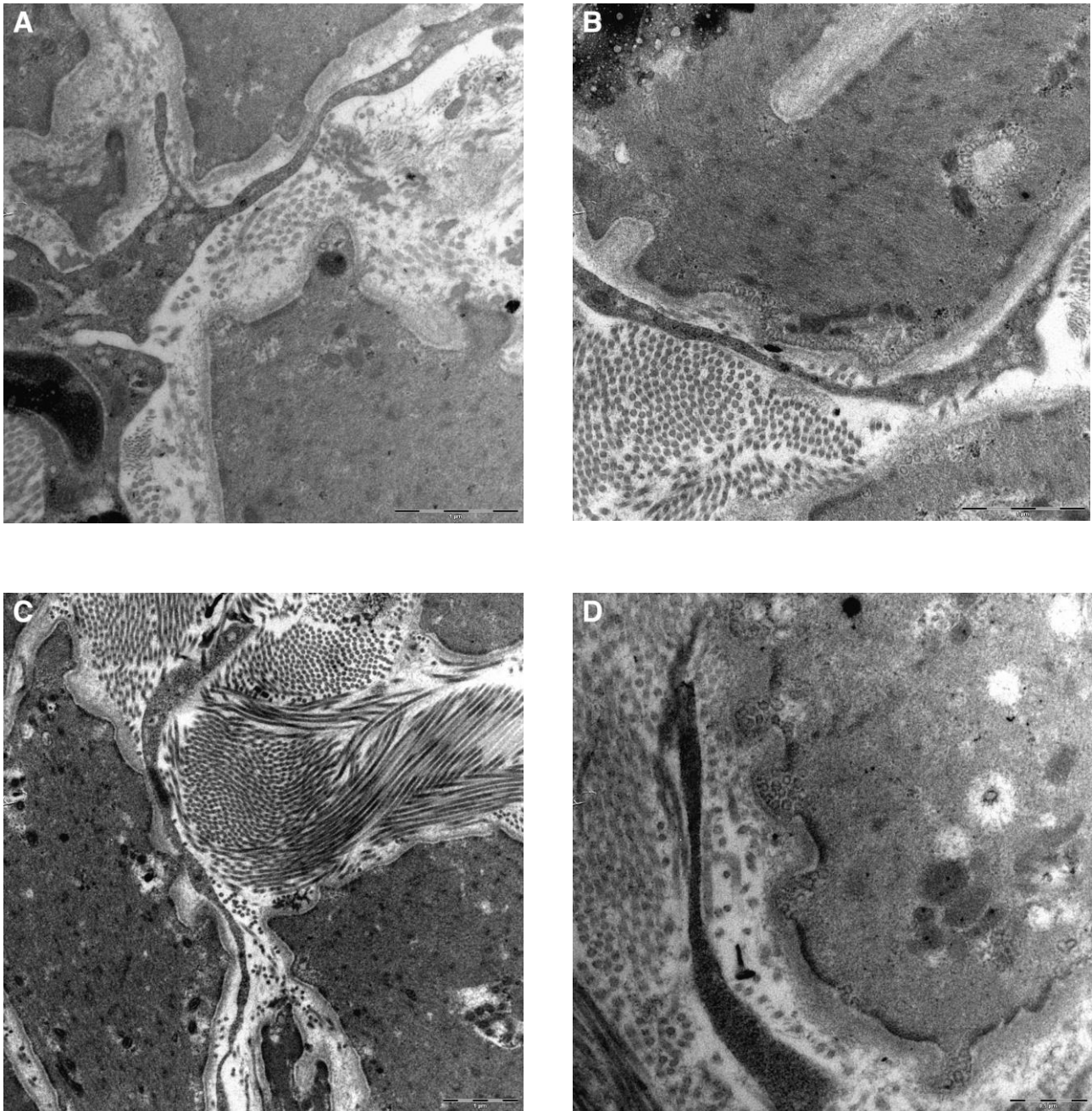


Fig. 10: TEM studies of ICLC processes in the media of lymphatic collectors.

A) ICLC with slender cell body and several cytoplasmic processes running between SMCs. Note blunt peg-like projections from SMC towards ICLC process. Bar = 1 μm .

B-C) Long processes of ICLC in close contact to SMCs. Note the accumulation of caveolae in SMC adjacent to the ICLC. Bar = 1 μm .

D) Higher magnification showing peg-like protrusions of SMC with caveolae. Bar = 0.5 μm

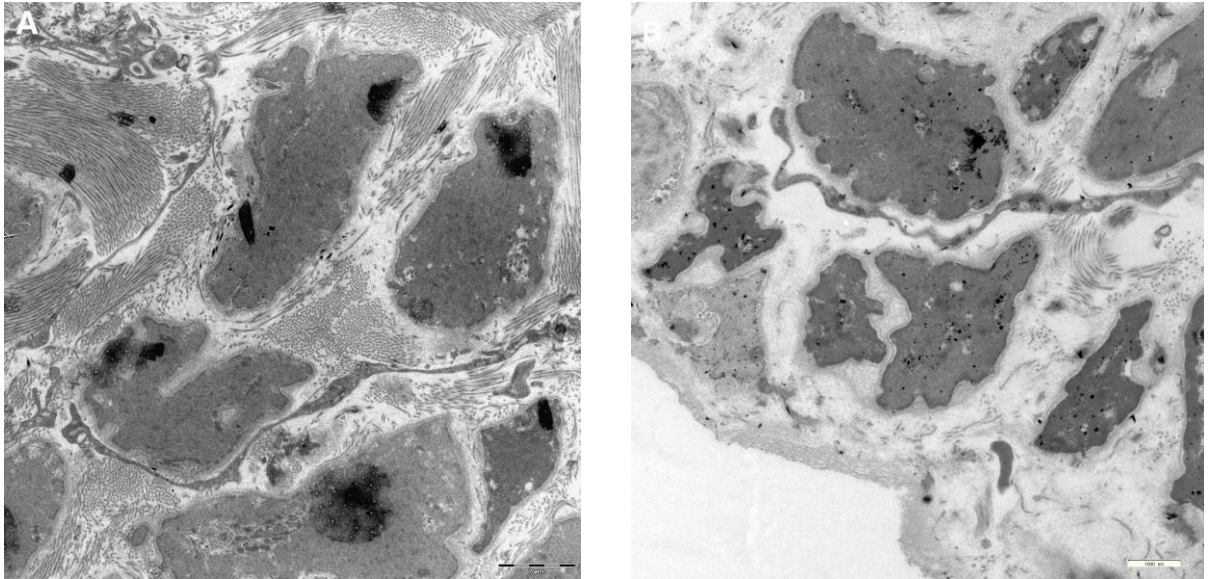


Fig. 11: TEM studies of ICLC processes in the media of lymphatic collectors.

A) Several long processes of ICLCs running between SMCs and connective tissue. Several dilatations (Ca^{2+} -handling units) along ICLC processes are seen. Bar = 2 μm

B) Long processes of ICLCs are running between SMCs. Note peg-like protrusions of SMCs towards ICLC processes. Bar = 1000 nm

3.2.5 Tunica media: Connective tissue

Depending on the caliber of the lymphatic collector, the amount of connective tissue varied. Essentially, three categories of fibers were found in the lymphatic collectors; collagenous, elastic and reticular (**Figs. 12, 13**). The proportions varied with vessel caliber and subsequent function. The larger caliber vessels, which are responsible for transporting large amounts of lymph and need to expand, showed more elastic fibers than the smaller vessels.

Collagen fibers were located throughout the media and adventitia of the lymphatic collectors. Fibers were observed oriented longitudinally, obliquely and transversely to the direction of the specimen section, which was usually transverse. The individual

collagen fiber widths varied between 45 nm and 65 nm. In the tunica media, collagen fibers were interspersed between SMC. Collagen fibers in the adventitia were found in bundles oriented in all directions.

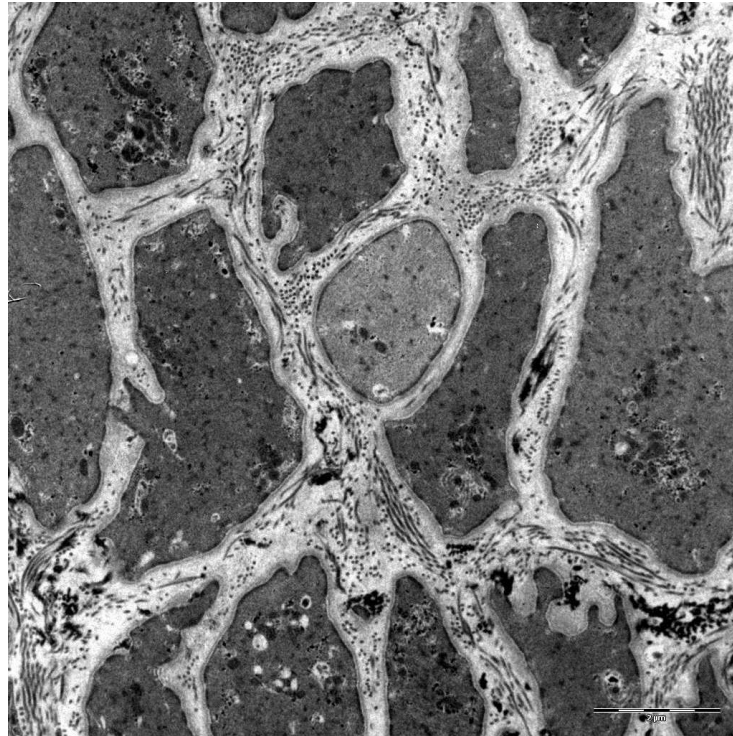


Fig. 12: Ultra-thin section of human epifascial lymphatic collector media connective tissue.

Collagen fibers interspersed between SMCs. Many are oriented longitudinally with the SMCs while others have a diagonal or transverse orientation. Bar = 2 μm

Elastic fibers were observed in large proportions mainly in the largest collectors throughout the tunica media. Smaller vessels had significantly less elastic fibers present. The elastic fibers of the larger vessels varied in size, some were only 0.7 μm wide while others measured 3 μm in diameter. They were interspersed between SMCs and collagenous fibers. Some fibers were surrounded by projections of fibroblasts.

Reticular fibers were found as part of the basement membrane meshwork under the endothelial cells.

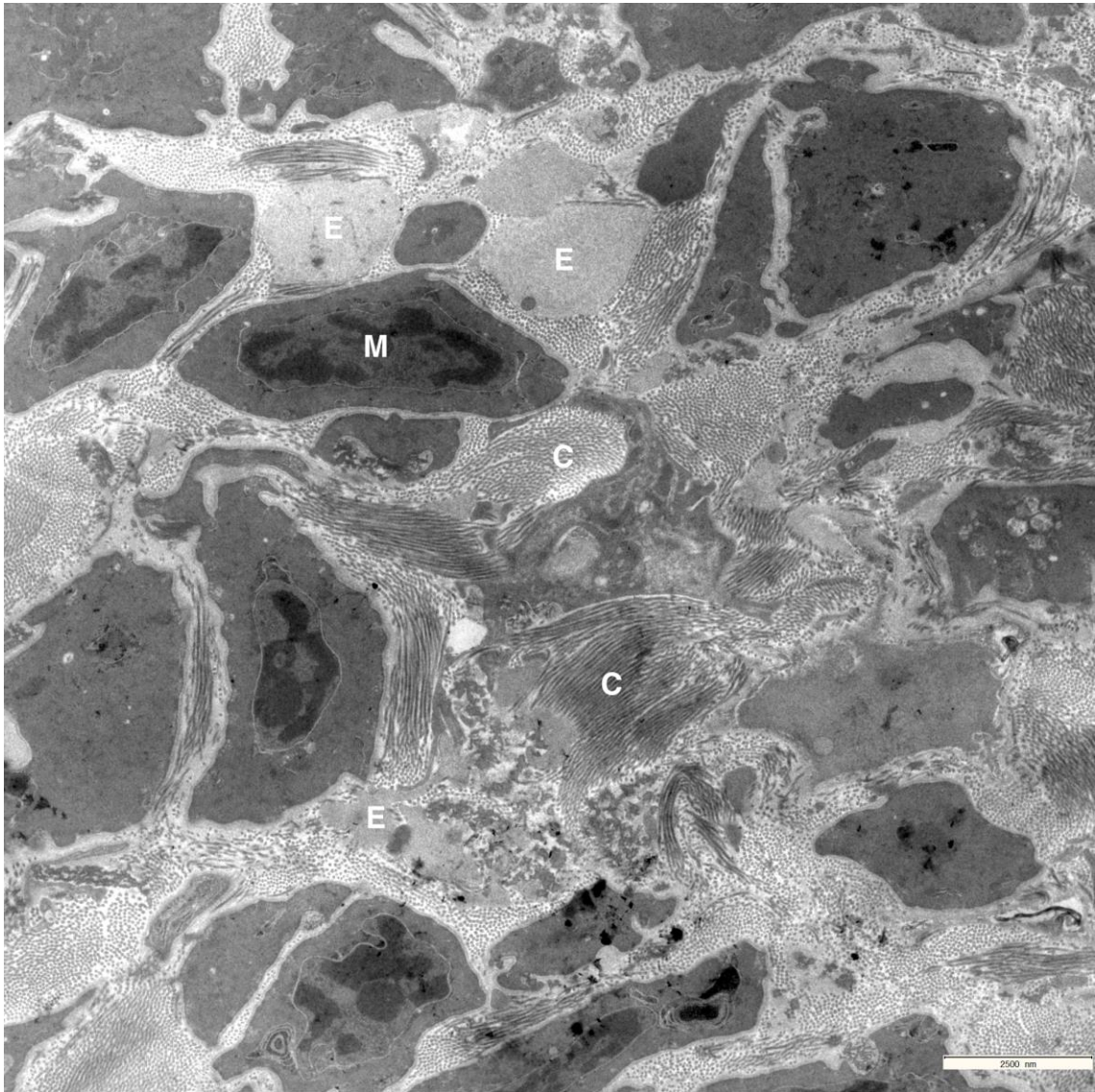


Fig. 13: Ultra-thin section of human epifascial lymphatic collector media containing elastin.

TEM picture of the media showing SMC (M), collagen bundles (C) and elastin (E). Varying amounts of elastin are dispersed amongst the collagen fibers and SMC. Bar = 2500 nm

3.2.6 Tunica externa

The adventitia was constructed of loose connective tissue. Many different structures were observed in this layer including blood vessels, mast cells, lipocytes, fibrocytes, and an abundance of collagen fibers (Figs. 14-16). Sparse numbers of axons were identified by immunohistology (not shown in my thesis), but could hardly be found in the TEM.

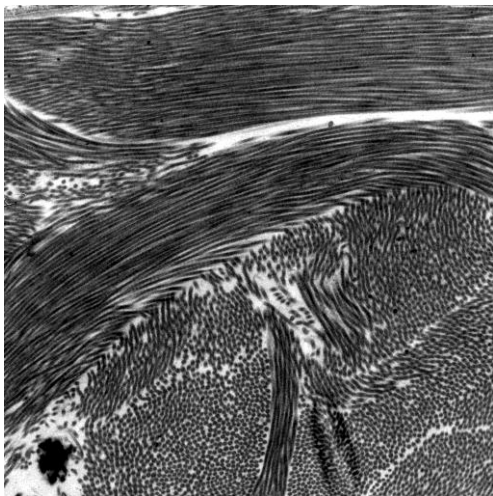


Fig. 14: Ultra-thin section of human epifascial lymphatic collector adventitia collagen. Collagen bundles are located in the adventitia with longitudinal and circumferential orientation. Bar = 1 μ m

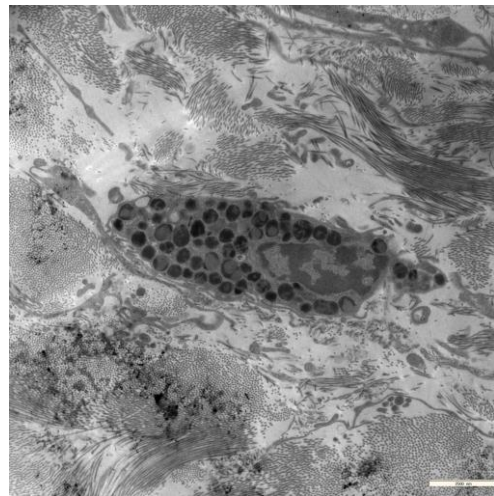


Fig. 15: Ultra-thin section of human epifascial lymphatic collector adventitia containing mast cell. Granulated mast cell located in the adventitia. Bar = 2500 nm

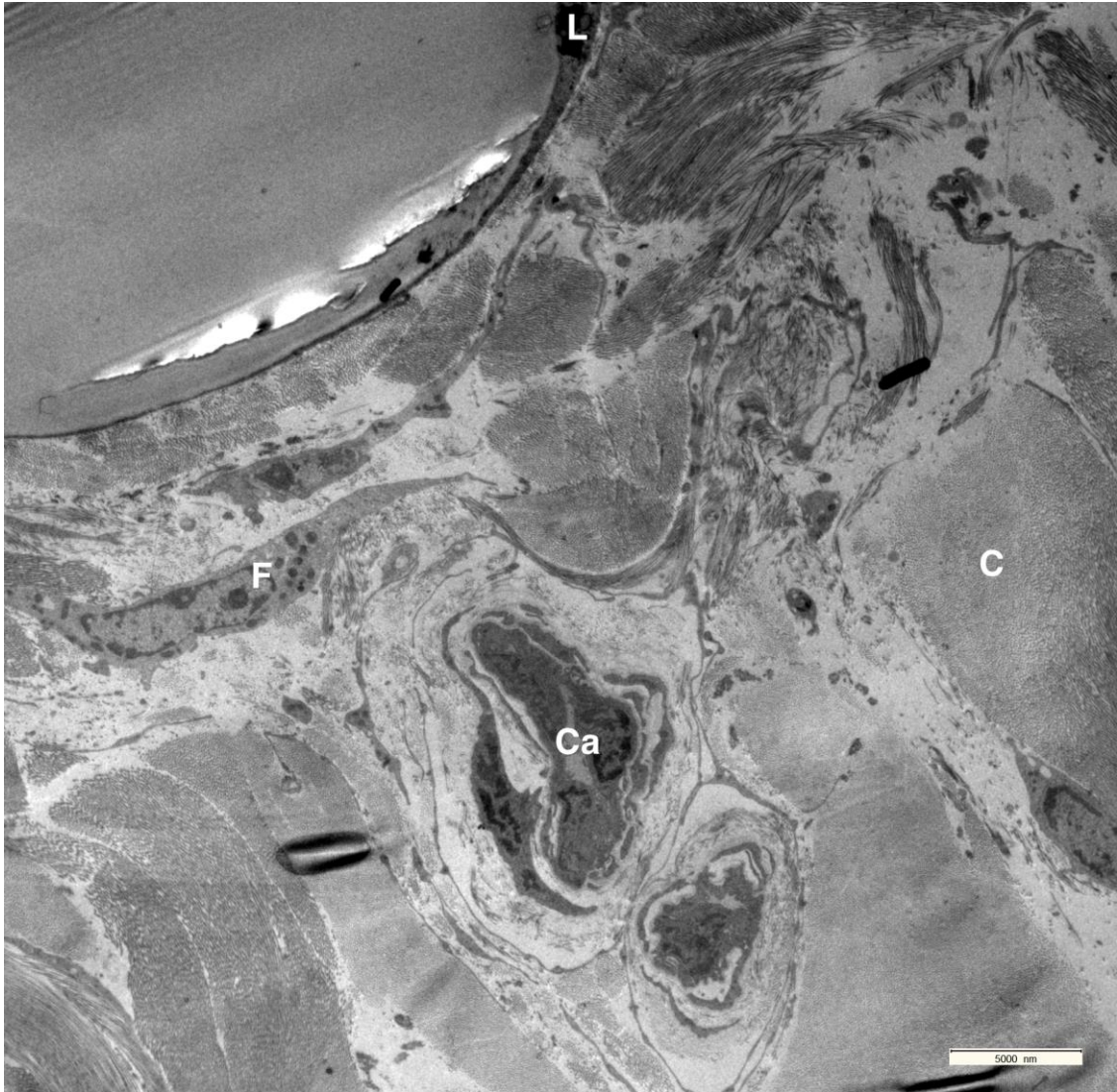


Fig. 16: Ultra-thin section of human epifascial lymphatic collector adventitia.

TEM picture of the adventitia containing lipocytes (L), capillaries (Ca), fibrocytes (F) and collagen bundles (C). Bar = 5000 nm

3.2.7 Fibrocytes compared to Interstitial Cajal-like Cells

Compared to ICLCs, fibrocytes had more cytoplasm surrounding their nucleus, were less elongated, contained abundant rough endoplasmatic reticulum and the nucleus contained mostly euchromatin (**Fig. 17**). Fibrocytes were abundantly found in the adventitia.



Fig. 17: Ultra-thin section of human epifascial lymphatic collector adventitia with fibrocyte.

Closer view of fibrocyte in Fig.16. The fibrocyte shows more cytoplasm surrounding its nucleus and more mitochondria than were seen in ICLCs. The processes are less elongated and gradually develop, in contrast to the processes of ICLCs that become thin very close to the cell body. F = fibrocyte; Ca = capillary. Bar = 5000 nm

4 Discussion

Until now, there hasn't been a detailed description of the ultrastructure of human lymphatic collectors. Here, the presence of lymphatic collectors has been shown with the injection of Patent Blue® intradermally into the first and second interdigital space, in order to identify the collectors of the patient's thigh. The injection of indocyanine green (ICG) and the use of infrared cameras have shown the active pumping of human dermal lymphatic collectors (Rasmussen et al. 2009). Briggs Boedtkjer et al. (2013) described the ultrastructure of the human thoracic duct. My thesis aimed to characterize the ultrastructure of epifascial human lymphatic collectors.

4.1 Mechanical concept of human lymphatic vessel contractility

Research has shown that lymphatic collectors possess autonomous peristaltic contractility, however, the pace-maker cells that potentially trigger these contractions of the SMC have not been undoubtedly identified (Witte et al. 2006). Theories to the contractility of lymphatic vessels started off as simply mechanical ones. In 1959, Horstmann conducted studies on guinea pig mesenteric lymph ducts. He argued that the contractions seen in lymph vessel segments were of mechanical nature (Horstmann 1959). He suggested that the mechanical functional unit consisted of the valve and the preceding segment of vessel because of the scarcity of smooth muscle cells in the valvular region. When one of these segments filled with lymph fluid, the musculature would be triggered to contract, propelling the fluid forward into the next segment. This segment would then contract due to distention and so on, thereby propelling fluid along the lymphatic vessel. Research since then has shown that the process is more complex and involves more than just the smooth muscle cells.

4.2 Physiological studies

Specifically, physiological studies on bovine and sheep mesenteric lymphatics have shown that even without intraluminal distention (Mawhinney and Roddie 1973) or with cutting off fluid input (McHale and Thornbury 1986), contractions of the vessels still occur. This strongly suggests the presence of some form of electrical pace-making initiating the contractions. The injection of indocyanine green (ICG) can elegantly show the active pumping of human dermal lymphatic collectors. The contractions and lymph flow can be observed with an infrared camera (Rasmussen et al. 2009).

4.3 Immuno-histological and ultra-structural identification of ICLC

McCloskey et al. found sub-endothelial cells in sheep, which could potentially be pace-maker cells. These cells stained positively for vimentin and c-kit (McCloskey et al. 2002). The cells were named Interstitial Cajal-like cells due to their similar appearance to the interstitial cells of Cajal found in the gastro-intestinal tract.

Interstitial Cajal-like cells (ICLCs) have been studied and described in various human body tissues including myocardium (S. Kostin, L. M. Popescu. 2009), resting mammary gland stroma (Gherghiceanu and Popescu 2005), uterus and fallopian tube (Popescu et al. 2007), and urinary bladder (Johnston et al. 2010) as well as in the largest part of the lymphatic system, the thoracic duct (Briggs Boedtkjer et al. 2013). More specifically, Briggs Boedtkjer et al. showed ICLCs to be located in the outer layer of SMC (Briggs Boedtkjer et al. 2013). Popescu et al. published a table containing criteria for the ultrastructural diagnosis of ICLCs and designated it the

“platinum standard” (Popescu et al. 2007). The criteria of this table coincide with the cells found in my research that I have designated to be ICLCs (Table 3).

ICLCs were identified ultrastructurally as ramified cells whose nuclei were surrounded by a slender perinuclear body, had an indented nucleus, and contained a low amount of caveolae and long cytoplasmic processes. These processes varied in caliber, were often in close contact with SMC and contained ‘varicous’ dilations along the processes. The areas of close contact between ICLC processes and SMCs showed a dense facing with caveolae at the contact sites. A patchy basal lamina was not observed as described in research on the thoracic duct (Briggs Boedtkjer et al. 2013).

It will require further research beyond the histological structure of the ICLC to fully understand its function and interaction with surrounding cells. Understanding the exact mechanism of communication between the ICLCs and the SMCs will be essential to developing treatment option for patients where this signaling pathway is defective.

Ultra-structural features	Characteristics
---------------------------	-----------------

1. Location	in the non-epithelial space
2. Close contact with targets	nerve bundles, and/or epithelia, and/or smooth muscle cells, and/or capillaries
3. Characteristic cytoplasmic processes	(1-5, frequently: 2-3) (tens up to hundreds of μm) (uneven caliber, $<0.5 \mu\text{m}$); <i>moniform</i> , usually with mitochondria in dilations present dichotomous pattern labyrinthic system of overlapping cytoplasmic processes
i. Number	
ii. Length	
iii. Thickness	
iv. Aspect	
v. "Ca ²⁺ release units"	
vi. Branching	
vii. Organization in network	dichotomous pattern labyrinthic system of overlapping cytoplasmic processes
4. Gap junctions	With smooth muscle cells or with each other
5. Basal lamina	occasionally present
6. Caveolae	2-4 % of cytoplasmic volume; ~ 0.5 caveolae/ μm of cell membrane length
7. Mitochondria	5-10 % of cytoplasmic volume
8. Endoplasmic reticulum	About 1-2 %, either smooth or rough
9. Cytoskeleton	<i>intermediate</i> and <i>thin filaments</i> , as well as <i>microtubules</i>
10. Myosin thick filaments	undetectable

Table 3: Interstitial tissue of the thigh lymphatic collector contains cells that meet the criteria for interstitial Cajal-like cells (Popescu et al. 2007)

(Usage of this table was kindly permitted by Sandra Maria Cretoiu (Ciontea))

5 Summary

The lymphatic vascular system is an important part of the body that still requires extensive research. Although great advances have been made over the past 20 years, many more will have to take place in order to fully understand the parts that make this system function. Gaining knowledge on the anatomy, histology, physiology and molecular biology will be important in creating cures and treatment options for patient suffering from lymphatic diseases such as lymphedema and in understanding the diseases as such.

The research that I have performed has added to the knowledge of the histological composition of the lymphatic collector. In particular, I was interested in establishing the presence of the interstitial Cajal-like cells ultra-structurally as the possible pacemaker of the lymphatic contractions, after the ICLCs had been identified in the largest lymphatic vessel, the thoracic duct.

I was able to verify that the general structure of the lymphatic collector is similar to that of the previously described thoracic duct (Briggs Boedtkjer et al. 2013) and the generally accepted structure of blood vessels, but also shows specific differences. The collectors contained a tunica interna (intima), tunica media and tunica externa (adventitia). The intima consisted of lymphatic endothelial cells. Unlike endothelial cells of larger blood vessels, however, the LECs were usually not resting on a sub-endothelial tissue layer, but were in close contact with smooth muscle cells. The tunica media was of variable thickness and contained smooth muscle cells (SMCs). I observed SMCs of light and dark cytoplasm, while both contained typical features such as dense bodies, caveolae and a basal lamina. Further research is required to establish a reason for this difference in appearance. It probably is a physiological sign

for a difference in function, similar to that of modified cardiac muscle cells with pacemaker and conducting functions in the heart.

Unlike what was observed by Boggon and Palfrey (1973) in their study of the microscopic anatomy of the human lymphatic trunk, I was able to find elastic fibers amongst the SMCs of the media, and also very clearly showed the presence of *vasa vasorum* throughout the media.

The adventitia layer of the lymphatic collectors was mainly composed of collagen fibers organized in bundles running obliquely or circumferentially. Fibroblasts were also frequently observed. Occasionally, scattered cells such as mast cells were found. Blood vessels and adipocytes were also seen in close approximation to the lymphatic collectors.

The discovery of ICLCs in the lymphatic collectors and their relationship to the surrounding SMCs was the main purpose of this thesis. In using the proposed criteria for ICLC identification put forth by Popescu et al. (2007), I was able to ultrastructurally identify ICLCs in the lymphatic collector. The discovery of a dense caveolar facing on the SMC membrane that was in close contact with the process of an ICLC opens up the possibility of communication via caveolae between the two cell types in order to initiate contractions. Now that the existence of ICLCs in the lymphatic collectors and lymphatic trunks has been established, it is necessary to find out how they function and communicate with SMCs, in order to learn how to influence them.

6 Appendix

6.1 List of Figures

Fig. 1: Immunofluorescence studies of epifascial lymphatic collectors from the human thigh	22
Fig. 2: TEM studies of epifascial lymphatic collector endothelial cells	25
Fig. 3: Ultra-thin section of human epifascial lymphatic collector endothelial cell.....	26
Fig. 4: Ultra-thin section of human epifascial lymphatic collector	27
Fig. 5: Magnified ultra-thin section of human epifascial lymphatic collector endothelial cell.....	27
Fig. 6: Ultra-thin sections of human epifascial lymphatic collectors smooth muscle cells.....	29
Fig. 7: Ultra-thin sections of human epifascial lymphatic collector LEC/SMC and smooth muscle cell connections	30
Fig. 8: Ultra-thin sections of human epifascial lymphatic collector vasa vasorum	31
Fig. 9: TEM studies of ICLCs in the media of lymphatic collectors	33
Fig. 10: TEM studies of ICLC processes in the media of lymphatic collectors.....	34
Fig. 11: TEM studies of ICLC processes in the media of lymphatic collectors.....	35
Fig. 12: Ultra-thin section of human epifascial lymphatic collector media connective tissue	36
Fig. 13: Ultra-thin section of human epifascial lymphatic collector media containing elastin.....	37
Fig. 14: Ultra-thin section of human epifascial lymphatic collector adventitia collagen	38
Fig. 15: Ultra-thin section of human epifascial lymphatic collector adventitia	

containing mast cell.....	38
Fig. 16: Ultra-thin section of human epifascial lymphatic collector adventitia.....	39
Fig. 17: Ultra-thin section of human epifascial lymphatic collector adventitia with fibrocyte	40

6.2 List of Tables

Table 1: Sequence for hematoxylin-eosin stain	14
Table 2: Contrast sequence for copper apertures	21
Table 3: Interstitial tissue of the thigh lymphatic collector contains cells that meet the criteria for interstitial Cajal-like cells	44

6.3 List of Abbreviations

BSA	Bovine serum albumin
Dapi	4',6-diamidino-2-phenylindol
DDSA	Dodecyl succinic anhydride
DMP	2,4,6-Tris(dimethylaminomethyl)phenol
HCL	Hydrochloric acid
H ₂ O	Dihydrogen monoxide
ICG	Indocyanine green
ICLC	Interstitial Cajal-like cells
KH ₂ PO ₄	Monopotassium phosphate
K ₂ HPO ₄	Dipotassium phosphate
LEC	Lymphatic endothelial cells

MNA	Methylnacid anhydride
$\text{Na}_3(\text{C}_6\text{H}_5\text{O}_7)$	Sodium citrate
NaOH	Sodium hydroxide
NaH_2PO_4	Monosodium phosphate
Na_2HPO_4	Disodium phosphate
OsO_4	Osmium tetroxide
$\text{Pb}(\text{NO}_3)_2$	Lead nitrate
PFA	Paraformaldehyde
PBS	Phosphate-buffered saline
PPB	Potassium phosphate buffer
SMC	Smooth muscle cell

7 Bibliography

Alessandrini C, Gerli R, Sacchi G, Ibba L, Pucci AM, Fruschelli C (1981):

Cholinergic and adrenergic innervation of mesenterial lymph vessels in guinea pig. *Lymphology* 14, 1-6

Allen JM, McCarron JG, McHale NG, Thornbury KD (1988): Release of [3H]-

noradrenaline from the sympathetic nerves to bovine mesenteric lymphatic vessels and its modification by alpha-agonists and antagonists. *Br J Pharmacol* 94, 823-833

Baluk P, Fuxe J, Hashizume H, Romano T, Lashnits E, Butz S, Vestweber D, Corada

M, Molendini C, Dejana E, McDonald DM (2007): Functionally specialized junctions between endothelial cells of lymphatic vessels. *J Exp Med.* 204(10), 2349-62

Berens von Routenfeld D, Drenckhahn D: Bau der Lymphgefäße. In: Drenckhahn D,

Zenker W (eds.): Benninghoff Anatomie: Mikroskopische Anatomie.

Embryologie und Histologie des Menschen. Urban & Schwarzenberg, München
1994, 756-761

Betterman KL, Harvey NL (2016): The lymphatic vasculature: development and role

in shaping immunity. *Immunol Rev* 271, 276–292

Boggon RP, Palfrey AJ (1973): The microscopic anatomy of human lymphatic trunks.

J Anat 114, 389-405

- Briggs Boedtkjer D, Rumessen J, Baandrup U, Skov Mikkelsen M, Telinius N, Pilegaard H, Aalkjaer C, Hjortdal V (2013): Identification of interstitial Cajal-like cells in the human thoracic duct. *Cells Tissues Organs* 197(2), 145-58
- Casley-Smith JR (1980): The fine structure and functioning of tissue channels and lymphatics. *Lymphology* 12, 177-183
- Felmerer G, Sattler T, Lohrmann C, Tobbia D (2012): Treatment of various secondary lymphedemas by microsurgical lymph vessel transplantation. *Microsurgery* 32(3), 171-177
- Gherghiceanu M, Popescu L M (2005): Interstitial Cajal-like cells (ICLC) in human resting mammary gland stroma. Transmission electron microscope (TEM) identification. *J Cell Mol Med* 9, 893-910
- Hollywood MA, McHale NG (1994): Mediation of excitatory neurotransmission by the release of ATP and noradrenaline in sheep mesenteric lymphatic vessels. *J Physiol* 481, 415- 423
- Horstmann E (1959): Beobachtungen zur Motorik der Lymphgefäße. *Pflugers Arch* 269, 511-519
- Johnston L, Woolsey S, Cunningham RMJ, O’Kane H, Duggan B, Keane P, McCloskey KD (2010): Morphological expression of *KIT* positive interstitial cells of Cajal in human bladder. *J Urology* 184, 370-377
- Kostin S, Popescu LM (2009): A distinct type of cell in myocardium: interstitial Cajal-like cells (ICLCs). *J Cell Mol Med* 13, 295-308

- Leak LV, Burke JF (1968): Ultrastructural studies on the lymphatic anchoring filaments. *J Cell Biol* 36, 129-149
- Mawhinney HJ, Roddie IC (1973): Spontaneous activity in isolated bovine mesenteric lymphatics. *J Physiol* 229, 339–348
- McCloskey KD, Hollywood MA, Thornbury KD, Ward SM, McHale NG (2002): Kit-like immunopositive cells in sheep mesenteric lymphatic vessels. *Cell Tissue Res* 310, 77-84
- McHale NG, Thornbury KD (1986): A method for studying lymphatic pumping activity in conscious and anaesthetised sheep. *J Physiol* 378, 109–118
- Neligan P, Piller N, Masia J (eds.): *Lymphedema: Complete Medical and Surgical Management*. Quality Medical Publishing, CRC Press, Abingdon, UK 2015
- Parton RG and Simons K (2007): The multiple faces of caveolae. *Nat Rev Mol Cell Biol* 8(3), 185-194
- Popescu LM, Ciontea SM, Cretoiu D (2007): Interstitial Cajal-Like Cells in Human Uterus and Fallopian Tube. *Ann NY Acad Sci* 1101, 139–165
- Rasmussen JC, Tan IC, Marshall MV, Fife CE, Sevic-Muraca EM (2009): Lymphatic imaging in humans with near-infrared fluorescence. *Curr Opin Biotechnol* 20, 74-82
- Rusznayk I, Földi M, Szabó G: *Lymphologie. Physiologie und Pathologie der Lymphgefäße und des Lymphkreislaufes*. 2nd edition; Fischer, Stuttgart 1969

- Sabin FR (1902): On the origin of the lymphatics system from the veins and the development of the lymph hearts and the thoracic duct in the pig. *Am J Anat* 1, 367–389
- Sabin FR (1904): On the development of superficial lymphatics in the skin of the pig. *Am J Anat* 3, 183–195
- Tammela T, Alitalo K (2010): Lymphangiogenesis: Molecular mechanisms and future promise. *Cell* 140(4), 460-76
- Todd GL, Bernard GR (1973): The sympathetic innervation of the cervical lymphatic duct of the dog. *Anat Rec* 177, 303-315
- Van der Putte SC (1975): The development of the lymphatic system in man. *Adv Anat Embryol Cell Biol* 51, 3-60
- Wigle JT, Harvey N, Detmar M, Lagutina I, Grosveld G, Gunn MD, Jackson DG, Oliver G (2002): An essential role for Prox1 in the induction of the lymphatic endothelial cells phenotype. *EMBO J* 21, 1505-1513
- Wilting J, Chao TI: Integrated anatomy of the vascular system. In: Lanzer P (ed.): *Panvascular Medicine*. Vol. 1, 2nd edition; Springer Verlag, Heidelberg New York 2015, 193 – 242
- Wilting J, Papoutsi M, Becker J (2004): The lymphatic vascular system: secondary or primary? *Lymphology* 31, 98-106
- Witte MH, Bernas MJ, Martin CP, Witte CL (2001): Lymphangiogenesis and lymphangiodysplasia: from molecular to clinical lymphology. *Microsc Res Tech* 55(2), 122-45

Witte MH, Jones K, Wilting J, Dictor M, Selg M, McHale N, Gershenwald JE,
Jackson DG (2006): Structure function relationships in the lymphatic system
and implications for cancer biology. *Cancer Metastasis Rev* 25(2), 159-84

Acknowledgements

I thank Prof. Dr. Jörg Wilting for giving me the opportunity and inspiration for this thesis and his support throughout.

I thank Dr. med. T. Ivo Chao for his support and helpful advice.

I am very grateful to Mrs. Ch. Zelent, Mrs. S. Hellbach, Mrs. S. Schwoch and Mr. B. Manshausen for their patience, support and excellent technical assistance.

I thank my sister Karoline Hasselhof for helping me acquire necessary research material.

Curriculum Vitae

I was born in Kiel, Germany on January 29th, 1990 as the second oldest child to Gert and Söhnke Hasselhof. We immigrated to Milwaukee, Wisconsin, USA in 1993. We moved several times within the state before ultimately settling in Muscoda, Wisconsin. That is where I attended school kindergarten through graduating from Riverdale High School as valedictorian in 2008. I attended the University of Wisconsin in Madison for the last semester of my senior year of high school before starting as a freshman of college in the fall of 2008. I completed my freshman year there before moving to Göttingen, Germany to attend the Medical University of Göttingen starting with the fall semester of 2009/2010. I completed the first state examination in 2011. One of the most rewarding electives I partook in was a month long stay in Accra, Ghana, working in the Korle-Bu Teaching Hospital. I completed my internship year at the University Hospital in Göttingen as well as the St. Berward Hospital in Hildesheim, Germany. Throughout my medical school journey, I had the pleasure and honor of working with amazing doctors, who mentored me and showed me what it means to be a great doctor. I passed the first part of the second state exam in 2013 and simultaneously passed the second part and graduated in November 2015.